Optical rotatory dispersion of methyloxirane in aqueous solution: assessing the performance of density functional theory in combination with a fully polarizable QM/MM/PCM approach

Franco Egidi,[1,2] **Ivan Carnimeo,**[3] **and Chiara Cappelli**[2,*]

[1]*Scuola Normale Superiore, Piazza dei Cavalieri, 7 I-56126 Pisa, Italy*
[2]*Dipartimento di Chimica e Chimica Industriale, Università di Pisa, via Giuseppe Moruzzi, 3 I-56124 Pisa, Italy*
[3]*Compunet, Istituto Italiano di Tecnologia (IIT), via Morego, 30 I-16163 Genova, Italy and Scuola Normale Superiore, Piazza dei Cavalieri, 7 I-56126 Pisa, Italy*

[*]*chiara.cappelli@unipi.it*

Abstract: We report a study on the performance of a recently developed fully polarizable QM/MM/PCM approach based on Fluctuating Charges (FQ) combined with 11 different Density Functionals for the description of the Optical Rotation at different wavelengths of (R)-Methyloxirane in aqueous solution. The results are compared with those obtained for the isolated system and for the solvated one as described by the Polarizable Continuum Model. In all cases, a comparison with experimental data is also shown. The results show that the effect of the solvent is much more significant than the effect of the density functional.

OCIS codes: (160.1585) Chiral media; (300.0300) Spectroscopy; (160.4760) Optical properties.

References and links

1. T. Crawford, "Ab initio calculation of molecular chiroptical properties," Theor. Chem. Acc. **115**, 227–245 (2006).
2. J. Autschbach, "Ab initio electronic circular dichroism and optical rotatory dispersion: From organic molecules to transition metal complexes," in *Comprehensive Chiroptical Spectroscopy, vol. 1,* , N. Berova, P. Polavarapu, K. Nakanishi, and R. W. Woody, eds. (Wiley, 2012), pp. 593–642.
3. T. D. Crawford, "High-accuracy quantum chemistry and chiroptical properties," in *Comprehensive Chiroptical Spectroscopy, vol. 1,* , N. Berova, P. Polavarapu, K. Nakanishi, and R. W. Woody, eds. (Wiley, 2012), pp. 675–697.
4. L. Goerigk, H. Kruse, and S. Grimme, "Theoretical electronic circular dichroism spectroscopy of large organic and supramolecular systems," in *Comprehensive Chiroptical Spectroscopy, vol. 1,* , N. Berova, P. Polavarapu, K. Nakanishi, and R. W. Woody, eds. (Wiley, 2012), pp. 643–674.
5. N. Berova, P. L. Polavarapu, K. Nakanishi, and R. W. Woody, eds. *Comprehensive Chiroptical Spectroscopy*, (Wiley, New York, 2012).
6. S. Superchi, C. Rosini, G. Mazzeo, and E. Giorgio, "Determination of molecular absolute configuration: Guidelines for selecting a suitable chiroptical approach," in *Comprehensive Chiroptical Spectroscopy, vol. 2,* , N. Berova, P. Polavarapu, K. Nakanishi, and R. W. Woody, eds. (Wiley, 2012), pp. 421–448.
7. M. Pecul and K. Ruud, "Solvent effects on natural optical activity," in *Continuum Solvation Models in Chemical Physics,* , B. Mennucci and R. Cammi, eds. (Wiley, New York, 2007), chap. 1.4, pp. 64–81.

#225483 - $15.00 USD Received 27 Oct 2014; revised 28 Nov 2014; accepted 28 Nov 2014; published 23 Dec 2014

8. F. Egidi, V. Barone, J. Bloino, and C. Cappelli, "Toward an accurate modeling of optical rotation for solvated systems: Anharmonic vibrational contributions coupled to the polarizable continuum model," J. Chem. Theory Comput. **8**, 585–597 (2012).
9. P. Mukhopadhyay, G. Zuber, M.-R. Goldsmith, P. Wipf, and D. N. Beratan, "Solvent effect on optical rotation: A case study of methyloxirane in water," ChemPhysChem **7**, 2483–2486 (2006).
10. M. Losada, P. Nguyen, and Y. Xu, "Solvation of propylene oxide in water: Vibrational circular dichroism, optical rotation, and computer simulation studies," J. Phys. Chem. A **112**, 5621–5627 (2008).
11. P. Mukhopadhyay, G. Zuber, P. Wipf, and D. Beratan, "Contribution of a solute's chiral solvent imprint to optical rotation," Angew. Chem., Int. Ed. **46**, 6450–6452 (2007).
12. J. Kongsted, T. B. Pedersen, M. Strange, A. Osted, A. E. Hansen, K. V. Mikkelsen, F. Pawlowski, P. Jørgensen, and C. Hättig, "Coupled cluster calculations of the optical rotation of s-propylene oxide in gas phase and solution," Chem. Phys. Lett. **401**, 385 – 392 (2005).
13. J. Kongsted and K. Ruud, "Solvent effects on zero-point vibrational corrections to optical rotations and nuclear magnetic resonance shielding constants," Chem. Phys. Lett. **451**, 226 – 232 (2008).
14. K. B. Wiberg, P. H. Vaccaro, and J. R. Cheeseman, "Conformational effects on optical rotation. 3-substituted 1-butenes," J. Am. Chem. Soc. **125**, 1888–1896 (2003).
15. K. Ruud and R. Zanasi, "The importance of molecular vibrations: The sign change of the optical rotation of methyloxirane," Angew. Chem., Int. Ed. **44**, 3594–3596 (2005).
16. B. C. Mort and J. Autschbach, "A pragmatic recipe for the treatment of hindered rotations in the vibrational averaging of molecular properties," ChemPhysChem **9**, 159–170 (2008).
17. J. Kongsted, T. B. Pedersen, L. Jensen, A. E. Hansen, and K. V. Mikkelsen, "Coupled cluster and density functional theory studies of the vibrational contribution to the optical rotation of (s)-propylene oxide," J. Am. Chem. Soc. **128**, 976–982 (2006).
18. M. C. Tam, N. J. Russ, and T. D. Crawford, "Coupled cluster calculations of optical rotatory dispersion of (s)-methyloxirane," J. Chem. Phys. **121**, 3550–3557 (2004).
19. T. J. Mach and T. D. Crawford, "Basis set dependence of coupled cluster optical rotation computations," J. Phys. Chem. A **115**, 10045–10051 (2011).
20. C. T. Campos, F. E. Jorge, T. P. Silva and M. R. Coppo, "Basis set convergence on optical rotation DFT calculations," Chem. Phys. Lett. **494**, 170–173 (2010).
21. J. Tomasi, B. Mennucci, and R. Cammi, "Quantum mechanical continuum solvation models," Chem. Rev. **105**, 2999–3093 (2005).
22. B. Mennucci, "Continuum Solvation Models: What Else Can We Learn from Them?" J. Phys. Chem. Lett. **1**, 1666–1674 (2010). And references therein.
23. F. Lipparini, F. Egidi, C. Cappelli, and V. Barone, "The optical rotation of methyloxirane in aqueous solution: a never ending story?" J. Chem. Theory Comput. **9**, 1880–1884 (2013).
24. F. Lipparini and V. Barone, "Polarizable force fields and polarizable continuum model: A fluctuating charges/PCM approach. 1. theory and implementation," J. Chem. Theory Comput. **7**, 3711–3724 (2011).
25. F. Lipparini, C. Cappelli, and V. Barone, "Linear response theory and electronic transition energies for a fully polarizable QM/classical hamiltonian," J. Chem. Theory Comput. **8**, 4153–4165 (2012).
26. F. Lipparini, C. Cappelli, G. Scalmani, N. De Mitri, and V. Barone, "Analytical first and second derivatives for a fully polarizable QM/classical hamiltonian," J. Chem. Theory Comput. **8**, 4270–4278 (2012).
27. F. Lipparini, C. Cappelli, and V. Barone, "A gauge invariant multiscale approach to magnetic spectroscopies in condensed phase: General three-layer model, computational implementation and pilot applications," J. Chem. Phys. **138**, 234108 (2013).
28. W. J. Mortier, K. Van Genechten, and J. Gasteiger, "Electronegativity equalization: application and parametrization," J. Am. Chem. Soc. **107**, 829–835 (1985).
29. S. W. Rick, S. J. Stuart, and B. J. Berne, "Dynamical fluctuating charge force fields: Application to liquid water," J. Chem. Phys. **101**, 6141–6156 (1994).
30. A. Rappe and W. Goddard, "Charge Equilibration for Molecular-Dynamics Simulations," J. Phys. Chem. **95**, 3358–3363 (1991).
31. A. D. Becke, "Density-functional thermochemistry. v. systematic optimization of exchange-correlation functionals," J. Chem. Phys. **107**, 8554–60 (1997).
32. H. L. Schmider and A. D. Becke, "Optimized density functionals from the extended g2 test set," J. Chem. Phys. **108**, 9624–31 (1998).
33. A. D. Becke, "Density-functional thermochemistry. III. the role of exact exchange," J. Chem. Phys. **98**, 5648–5652 (1993).
34. R. Peverati and D. G. Truhlar, "A global hybrid generalized gradient approximation to the exchange-correlation functional that satisfies the second-order density-gradient constraint and has broad applicability in chemistry," J. Chem. Phys. **135**, 191102 (2011).
35. C. Adamo and V. Barone, "Toward reliable density functional methods without adjustable parameters: The PBE0 model," J. Chem. Phys. **110**, 6158–6169 (1999).
36. Y. Zhao and D. G. Truhlar, "The M06 suite of density functionals for main group thermochemistry, thermochemi-

#225483 - $15.00 USD Received 27 Oct 2014; revised 28 Nov 2014; accepted 28 Nov 2014; published 23 Dec 2014

cal kinetics, noncovalent interactions, excited states, and transition elements: two new functionals and systematic testing of four M06-class functionals and 12 other functionals," Theor. Chem. Acc. **393**, 215–241 (2008).
37. C. Adamo and V. Barone, "Exchange functionals with improved long-range behavior and adiabatic connection methods without adjustable parameters: The mpw and mpw1pw models," J. Chem. Phys. **108**, 664–75 (1998).
38. T. Yanai, D. P. Tew, and N. C. Handy, "A new hybrid exchange-correlation functional using the coulomb-attenuating method (cam-b3lyp)," Chem. Phys. Lett. **393**, 51–57 (2004).
39. O. A. Vydrov and G. E. Scuseria, "Assessment of a long range corrected hybrid functional," J. Chem. Phys. **125**, 234109 (2006).
40. O. A. Vydrov, J. Heyd, A. Krukau, and G. E. Scuseria, "Importance of short-range versus long-range hartree-fock exchange for the performance of hybrid density functionals," J. Chem. Phys. **125**, 074106 (2006).
41. O. A. Vydrov, G. E. Scuseria, and J. P. Perdew, "Tests of functionals for systems with fractional electron number," J. Chem. Phys. **126**, 154109 (2007).
42. J. D. Chai and M. Head-Gordon, "Long-range corrected hybrid density functionals with damped atom-atom dispersion corrections," Phys. Chem. Chem. Phys. **10**, 6615–6620 (2008).
43. D. Jacquemin, M. Barry, II, A. Planchat, C. Adamo, and J. Autschbach, "Performance of an optimally tuned range-separated hybrid functional for 0-0 electronic excitation energies," J. Chem. Theory Comput. **10**, 1677–1685 (2014).
44. M. Biczysko, P. Panek, G. Scalmani, J. Bloino, and V. Barone, "Harmonic and anharmonic vibrational frequency calculations with the double-hybrid B2PLYP method: Analytic second derivatives and benchmark studies," J. Chem. Theory Comput. **6**, 2115–2125 (2010).
45. P. Carbonniere, T. Lucca, C. Pouchan, N. Rega, and V. Barone, "Vibrational computations beyond the harmonic approximation: Performances of the b3lyp density functional for semirigid molecules," J. Chem. Phys. **26**, 384–388 (2005).
46. P. Mukhopadhyay, G. Zuber, M.-R. Goldsmith, P. Wipf, and D. N. Beratan, "Solvent effect on optical rotation: A case study of methyloxirane in water," ChemPhysChem. **7**, 2483–2486 (2006).
47. R. A. Kendall, T. H. Dunning Jr., and R. J. Harrison, "Electron affinities of the first-row atoms revisited. systematic basis sets and wave functions," J. Chem. Phys. **96**, 6796–6806 (1992).
48. E. D. Hedegård, F. Jensen, and J. Kongsted, "Basis set recommendations for DFT calculations of gas-phase optical rotation at different wavelengths," J. Chem. Theory Comput. **8**, 4425–4433 (2012).
49. K. B. Wiberg, M. Caricato, Y.-G. Wang, and P. H. Vaccaro, "Towards the accurate and efficient calculation of optical rotatory dispersion using augmented minimal basis sets," Chirality **25**, 606–616 (2013).
50. A. Baranowska-czkowska and K. Z. czkowski, "The orp basis set designed for optical rotation calculations," J. Comput. Chem. **34**, 2006–2013 (2013).
51. E. Cancès, B. Mennucci, and J. Tomasi, "A new integral equation formalism for the polarizable continuum model: Theoretical background and applications to isotropic and anisotropic dielectrics," J. Chem. Phys. **107**, 3032–3041 (1997).
52. M. J. Frisch, G. W. Trucks, H. B. Schlegel, G. E. Scuseria, M. A. Robb, J. R. Cheeseman, G. Scalmani, V. Barone, B. Mennucci, G. A. Petersson, H. Nakatsuji, M. Caricato, X. Li, H. P. Hratchian, A. F. Izmaylov, J. Bloino, G. Zheng, J. L. Sonnenberg, M. Hada, M. Ehara, K. Toyota, R. Fukuda, J. Hasegawa, M. Ishida, T. Nakajima, Y. Honda, O. Kitao, H. Nakai, T. Vreven, J. A. Montgomery, Jr., J. E. Peralta, F. Ogliaro, M. Bearpark, J. J. Heyd, E. Brothers, K. N. Kudin, V. N. Staroverov, R. Kobayashi, J. Normand, K. Raghavachari, A. Rendell, J. C. Burant, S. S. Iyengar, J. Tomasi, M. Cossi, N. Rega, J. M. Millam, M. Klene, J. E. Knox, J. B. Cross, V. Bakken, C. Adamo, J. Jaramillo, R. Gomperts, R. E. Stratmann, O. Yazyev, A. J. Austin, R. Cammi, C. Pomelli, J. W. Ochterski, R. L. Martin, K. Morokuma, V. G. Zakrzewski, G. A. Voth, P. Salvador, J. J. Dannenberg, S. Dapprich, A. D. Daniels, Ö. Farkas, J. B. Foresman, J. V. Ortiz, J. Cioslowski, and D. J. Fox, "Gaussian Development Version Revision H.30," Gaussian Inc. Wallingford CT 2009.
53. H. Berendsen, D. van der Spoel, and R. van Drunen, "Gromacs: A message-passing parallel molecular dynamics implementation," Comp. Phys. Comm. **91**, 43 – 56 (1995).
54. E. Lindahl, B. Hess, and D. van der Spoel, "Gromacs 3.0: a package for molecular simulation and trajectory analysis," J. Mol. Model. **7**, 306–317 (2001).
55. D. Van Der Spoel, E. Lindahl, B. Hess, G. Groenhof, A. E. Mark, and H. J. C. Berendsen, "Gromacs: Fast, flexible, and free," J. Comput. Chem. **26**, 1701–1718 (2005).
56. B. Hess, C. Kutzner, D. van der Spoel, and E. Lindahl, "Gromacs 4: Algorithms for highly efficient, load-balanced, and scalable molecular simulation," J. Chem. Theory Comput. **4**, 435–447 (2008).
57. S. Miyamoto and P. A. Kollman, "Settle: An analytical version of the shake and rattle algorithm for rigid water models," J. Comput. Chem. **13**, 952–962 (1992).
58. U. Essmann, L. Perera, M. L. Berkowitz, T. Darden, H. Lee, and L. G. Pedersen, "A smooth particle mesh ewald method," J. Chem. Phys **103**, 8577–8593 (1995).
59. H. J. C. Berendsen, J. P. M. Postma, W. F. van Gunsteren, A. DiNola, and J. R. Haak, "Molecular dynamics with coupling to an external bath," J. Chem. Phys. **81**, 3684–3690 (1984).
60. W. L. Jorgensen, D. S. Maxwell, and J. Tirado-Rives, "Development and testing of the opls all-atom force field on conformational energetics and properties of organic liquids," J. Am. Chem. Soc. **118**, 11225–11236 (1996).

#225483 - $15.00 USD Received 27 Oct 2014; revised 28 Nov 2014; accepted 28 Nov 2014; published 23 Dec 2014

61. T. D. Crawford, M. C. Tam, and M. L. Abrams, "The current state of ab initio calculations of optical rotation and electronic circular dichroism spectra," J. Phys. Chem. A **111**, 12057–12068 (2007).
62. S. M. Wilson, K. B. Wiberg, J. R. Cheeseman, M. J. Frisch, and P. H. Vaccaro, "Nonresonant optical activity of isolated organic molecules," J. Phys. Chem. A **109**, 11752–11764 (2005).
63. F. Egidi, J. Bloino, V. Barone, and C. Cappelli, "Toward an accurate modeling of optical rotation for solvated systems: Anharmonic vibrational contributions coupled to the polarizable continuum model," J. Chem. Theory Comput. **8**, 585–597 (2012).
64. Y. Kumata, J. Furukawa, and T. Fueno, "The effect of solvents on the optical rotation of propylene oxide," Bull. Chem. Soc. Jpn. **43**, 3920–3921 (1970).
65. B. Mennucci, "Hydrogen bond versus polar effects: An ab initio analysis on n f * absorption spectra and N nuclear shieldings of diazines in solution," J. Am. Chem. Soc. **124**, 1506–1515 (2002).
66. C. Cappelli, S. Corni, B. Mennucci, R. Cammi, and J. Tomasi, "Vibrational Circular Dichroism within the Polarizable Continuum Model: A theoretical evidence of conformation effects and Hydrogen bonding for (S)-(-)-3-butyn-2-ol in CCl_4 solution," J. Phys. Chem. A **106**, 12331–12339 (2002).
67. C. Cappelli, B. Mennucci, and S. Monti, "Environmental effects on the spectroscopic properties of gallic acid: A combined classical and quantum mechanical study," J. Phys. Chem. A **109**, 1933–1943 (2005).
68. M. R. Poopari, Z. Dezhahang, and Y. Xu, "A comparative vcd study of methyl mandelate in methanol, dimethyl sulfoxide, and chloroform: explicit and implicit solvation models," Phys. Chem. Chem. Phys. **15**, 1655–1665 (2013).
69. M. R. Poopari, P. Zhu, Z. Dezhahang, and Y. Xu, "Vibrational absorption and vibrational circular dichroism spectra of leucine in water under different ph conditions: Hydrogen-bonding interactions with water," J. Chem. Phys. **137**, 194308 (2012).

1. Introduction

In the last decades Quantum-Mechanical (QM) methods have been amply applied to the calculation of chiroptical properties and spectroscopies [1–4]. The results that can nowadays be achieved are so reliable and accurate that QM protocols have become a powerful methodology to assist experimentalists in the reliable determination of the molecular absolute configuration [5, 6].

However, chiroptical properties and spectroscopies are usually measured for solutions or pure liquids, and this should be taken into account in the computational modeling, because the environment may affect not only the absolute value but especially the sign of the chiroptical response [5, 7]. The Optical Rotation (OR) of methyloxirane is a well known example of such a behavior and has been so far amply studied [8–17]. In particular, both the Coupled Cluster and Density Functional Theory (DFT) levels of theory have been employed and it has been reported [15–19] that DFT (with the B3LYP functional) combined with the aug-cc-pVDZ basis set gives electronic OR values comparable to Coupled Cluster Singles and Doubles (CCSD) with extended basis sets [19] for an incident wavelength of 589 nm, though this result is likely based on a cancellation of errors as Campos et al. [20] have shown that by increasing the size of the basis set there is a decrease in the agreement between the experimental and calculated OR using different DFT functionals.

However, both methods completely fail at describing the OR of methyloxirane in aqueous solution, even when coupled with implicit solvation models such as the Polarizable Continuum Model (PCM) [21,22]. In fact, a thorough study on solvent effects employing the PCM has been recently performed by some of the present authors [8], demonstrating that continuum solvation models can adequately describe solvent effects on OR when the dominating solvent contribution arises from bulk effects [8], whereas if specific solute-solvent interactions are present, they are not able to correctly reproduce the observed sign of the property.

A quantitative agreement with experiments in aqueous solution was however recently achieved by some of us [23], by exploiting an integrated QM/MM/PCM model, named QM/FQ/PCM, which combines a fluctuating charge (FQ) approach to the Molecular Mechanics (MM) polarization with the PCM [24–27]. In this model, polarization effects are considered by endowing each atom with a charge, which depends on the atomic electronegativity and

#225483 - $15.00 USD Received 27 Oct 2014; revised 28 Nov 2014; accepted 28 Nov 2014; published 23 Dec 2014

hardness [24], and which is obtained by resorting to the electronegativity equalization principle [28–30]. Due to the development and implementation of analytical first and second derivatives [26], response equations to electric [25] and magnetic perturbations with GIAOs [27], the QM/FQ/PCM model is currently able to describe chiroptical properties and spectroscopies, which are formally mixed electric-magnetic phenomena.

An issue which is still open is a general assessment of the quality of the coupling between the QM/FQ/PCM and DFT. In fact, as mentioned above, an exceptional agreement between calculations and experiments is achieved by exploiting the B3LYP and CAM-B3LYP functionals, however the general performance of different functionals has never been tested. In addition, the final OR which is predicted by this approach results from the average over a large number of snapshots extracted from Molecular Dynamics (MD) simulations [23]. We have found a really large variation of OR values around the average for the different snapshots (consisting of a few hundreds of solvent molecules), and it has not yet been assessed whether such a variation is related to the chosen functionals and whether a different choice would have led to different average values. In this paper we will investigate these points, and in particular we will report the results obtained by using 11 different functionals ranging from pure (B97D [31,32]), to different classes of hybrid functionals (B3LYP [33], SOGGA11-X [34], PBE0 [35], BHandHLYP [33], M06 [36], M06-2X [36], and mPW1PW91 [37]), including also long-range (CAM-B3LYP [38], LC-ωPBE [39–41]) and dispersion corrections (ωB97xD [42]). The current choice of functionals is also supported by the results reported in Ref. [43], where different functionals were tested for electronic transition energies.

The computational protocol which we will exploit follows the one successfully applied in a previous paper [23]. In particular, we will not limit the analysis to purely electronic effects, but anharmonic vibrational contributions, whose effect has demonstrated to be substantial [8, 13–17], will be added to the electronic property computed at the equilibrium geometry. Such corrections will account for solvent effects, by following the procedure already tested by some of us [8]. Since the motions of the solvent will be treated classically by means of MD simulations, vibrational corrections will be assumed to be independent of the solvent configurations and the MD simulation will be performed by freezing the (R)–methyloxirane geometry.

Therefore, the basic steps of the computational protocol are:

1. the geometry of (R)–methyloxirane is optimized accounting for the effects of the aqueous environment by means of the PCM at the B3LYP/aug-cc-pVDZ level. Indeed, such a combination of functional and basis set has been demonstrated to provide good geometries and vibrational properties for various isolated and solvated systems [44, 45]. Therefore, in order to avoid the inclusion of another parameter, which would complicate the comparison, all the calculations at the QM/FQ/PCM level will be done with the same geometry;

2. 2000 snapshots are extracted from an MD simulation performed by using a fixed methyloxirane geometry as obtained at step 1;

3. for each snapshot, a spherical cluster centered on the solute is cut and surrounded by a spherical PCM cavity. Thus system is then used to calculate the OR at the QM/FQ/PCM level;

4. the calculated OR is averaged over the snapshots and vibrational corrections calculated at the B3LYP/aug-cc-pVDZ/PCM level are added to the average value, similarly to what already reported [8].

In the following discussion, the results obtained with the QM/FQ/PCM approach will be compared to the corresponding QM calculation for the isolated system, the solvated one as

#225483 - $15.00 USD Received 27 Oct 2014; revised 28 Nov 2014; accepted 28 Nov 2014; published 23 Dec 2014

described by means of PCM and with experimental ORD curves [46].

2. Computational details

All the calculations were performed by using the aug-cc-pVDZ basis set [47], to keep our results in line with previously reported theoretical investigations. Notice that basis sets specifically optimized for the calculation of the OR have been reported [48–50].

Calculation in gas phase and with PCM were performed both by using the same geometry employed for the MD simulations [23] and by re-optimizing it at each level. PCM calculations were performed by exploiting the IEF-PCM implementation [51] with $\varepsilon = 78.3553$, $\varepsilon_\infty = 1.777849$ and Gaussian09 [52] defaults for the cavity shape and sphere radii.

Anharmonic vibrational corrections were taken from a previous study [8].

A 25 ns MD simulation of (R)–methyloxirane in a pre-equilibrated box of 2175 SPC water molecules was performed in the NPT ensemble using GROMACS [53–56]. The leapfrog integrator was used with a 1 fs time step. All bonds were kept rigid using the settle algorithm [57] for water; the geometry of the solute was kept rigid through all the simulation. For electrostatic interactions, the Particle-Mesh Ewald summation method was used [58]. The pressure was held at 1 bar using the weak-coupling scheme [59] with a coupling constant of 10 ps and an isotherm compressibility of 5 10^{-5} bar^{-1}. Each component of the system (i.e. methyloxirane and water) was coupled separately to a temperature bath at 300 K, using the Berendsen thermostat [59], with a coupling constant of 0.5 ps. The all-atoms OPLS-AA [60] force field was used for the solute. The methyloxirane optimized geometry in water already used in Ref. [23] was used, and kept fixed for the entire MD simulation.

2000 snapshots were extracted from the last 20 ns of the MD simulation (one snapshot every 10 ps). For each snapshot, a 12Å sphere centered in the solute's geometrical center was cut. A 1.5 Å larger radius was used for the PCM spherical cavity. For each snapshot, the OR of methyloxirane at different wavelengths was calculated with the QM/FQ/PCM model, using the SPC FQ parameters given by Rick et al. [29] and the PCM for bulk water. All the DFT calculations were done by using a locally modified version of the Gaussian09 package [52].

Al reported OR values are given in $deg\ dm^{-1}g^{-1}cm^3$.

3. Numerical results

We start the discussion of the results by analyzing ORD curves of methyloxirane in gas phase. This analysis is only intended to set a reference for the following discussion on the solvated system: the performance of DFT with respect to more accurate QM methodologies, such as Coupled Cluster approaches, for the calculation of the OR has already studied in detail in the literature [61]. Figure 1 shows ORD curves from 365 nm to 635 nm calculated by both fixing the methyloxirane geometry to the one later used for the MD simulations (panel a) and by re-optimizing it for each functional (panel b). The former serves as a direct reference for the data reported in the following discussion for the solvated system, in order to disentangle the effects of the geometry and those of the environment. Experimental gas-phase OR values measured by Vaccaro and coworkers [62] at 355 and 633 nm are also shown, as well as the entire ORD curve for methyloxirane dissolved in water solution [46]. By comparing panels a and b in Fig. 1, we note that the optimization of the geometry affects the OR absolute values, however the overall behavior of the ORD curve is the same. Experimental values in aqueous solution are always negative, whereas, judging from the two available data, gas phase values go from positive to negative as the wavelength decreases. Our calculated data are in all cases positive (with the exception of the B97D functional). More in detail, the increasing behavior of the experimental curve is not correctly reproduced by the M06-2X, LC-ωPBE, ωB97xD, BHandHLYP and SOGGA11-X functionals.

#225483 - $15.00 USD Received 27 Oct 2014; revised 28 Nov 2014; accepted 28 Nov 2014; published 23 Dec 2014

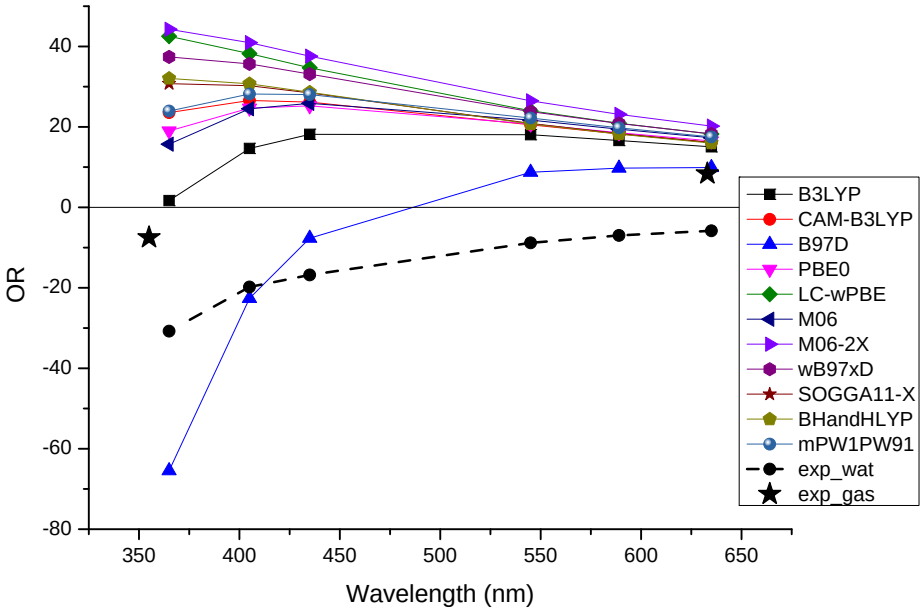

(a)

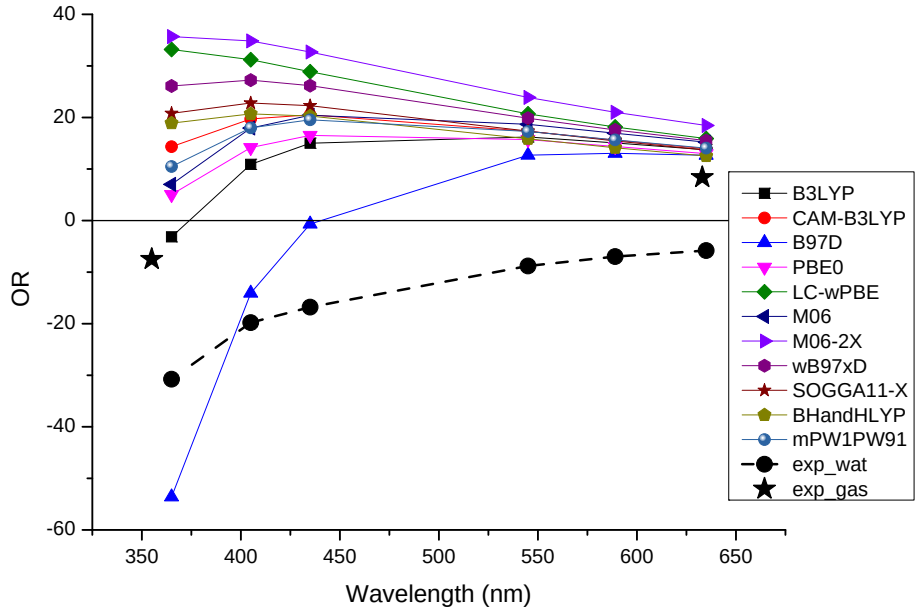

(b)

Fig. 1. ORD of (R)-methyloxirane in gas phase as calculated by exploiting different functionals and the aug-cc-pVDZ basis set. Top panel: fixed B3LYP/aug-cc-pVDZ/PCM geometry; bottom panel: optimized geometry in vacuo with each functional. Experimental values in gas phase [62] and the experimental ORD in aqueous solution [46] are also shown.

#225483 - $15.00 USD Received 27 Oct 2014; revised 28 Nov 2014; accepted 28 Nov 2014; published 23 Dec 2014

A slightly better performance is achieved by the other functionals, with B3LYP performing somewhat better than the rest. B97D (the only pure functional on the list) gives a very good prediction of the experimental value at 633 nm, and a correct sign for lower wavelengths, even though the absolute value at 355 nm is largely overestimated. This apparently better performance might however be due to the neglect of vibrational corrections which, for this system, have been shown to be negative [63]. Another explanation may stem from the fact that B97D gives the lowest first excitation energy among the tested functionals (data not shown), which causes a redshift in the pole of the response function.

Calculated PCM values are reported in Fig. 2. The upper panel (a) shows the values computed at the geometry later used for the MD simulation, the lower panel (b) shows the values computed after a geometry optimization, with PCM, for each functional. It can be seen that, in comparison with the gas phase values of Fig. 1, PCM generally lowers all curves, shifting them in the right direction with respect to experimental data, and brings the concavity of all curves downward. In either the fixed- or optimized-geometry plots, the sign of the OR is only reproduced for some functionals and only for lower wavelengths, reiterating the fact that the implicit description of the solute-solvent interaction is not adequate for the prediction of the OR of methyloxirane in water, even though it has been shown to be appropriate in the case of other solvents [63]. Moving to a more detailed analysis of the effects due to geometry optimization (see Fig. 3), we note they are not uniform across all functionals: for instance the mPW1PW91 and PBE0 functionals are influenced much more heavily than the SOGGA11-X by the geometry optimization. Four functionals (B3LYP, CAM-B3LYP. M06 and M06-2X) show a significant positive change, two (PBE0 and MPW1PW91) show a significant negative effect, whereas very small changes are noticed for the other hybrid functionals. B97D shows huge positive effects.

In Fig. 4 the difference between PCM and gas phase values, at respective equilibrium geometries are shown. Once again, B97D is visibly off. In general, a uniform and negative effect is noticed, and in all cases the extent of solvent effects largely overtakes those due to the choice of a different geometry for each functional (compare Fig. 3).

Finally, the values computed by exploiting the QM/FQ/PCM protocol are presented in Fig. 5. The upper panel (a) shows the electronic component of the OR, whereas the lower panel (b) includes anharmonic vibrational corrections computed for each wavelength at the B3LYP/aug-cc-pVDZ/PCM level of theory.

The extent of specific interaction is substantial, as it can be seen from the comparison with PCM values (Fig. 6). The shift is always negative, and its amount is of the same order of PCM calculated values. This finally results in a change of sign, which brings the calculated FQ/PCM values towards the experiment (see Fig. 5(a)). With the exception of LC-ωPBE, M06-2X, M06, and mPW1PW91, all other functionals achieve the correct sign of the OR at all wavelengths, whereas the aforementioned four functionals for the highest wavelengths still yield positive values, albeit very small. This qualitative picture does not significantly change upon addition of the vibrational correction (Fig. 5(b)), which lowers all curves by higher amounts the lower the wavelengths. At long wavelengths all functionals seem to overestimate the computed OR, however it should be mentioned that older experimental measurements for the OR of methyloxirane in water at 589 nm gave a less negative value of -4.3 [64]. At shorter wavelengths all functionals (with the exception of B97D) seem to cluster around the experimental value, with significant variation, and the best agreement is achieved by the BHandHLYP and SOGGA11-X functionals (Fig. 7). It should be mentioned that previous studies have shown that at low wavelengths the effect of the basis set is more significant, therefore the identification of the best functional might change if a more complete basis set were employed [48].

As last comment, Fig. 8 shows the standard deviation of the purely electronic FQ/PCM OR values at the different wavelengths across the 2000 snapshots. Note that since we are using the

#225483 - $15.00 USD Received 27 Oct 2014; revised 28 Nov 2014; accepted 28 Nov 2014; published 23 Dec 2014

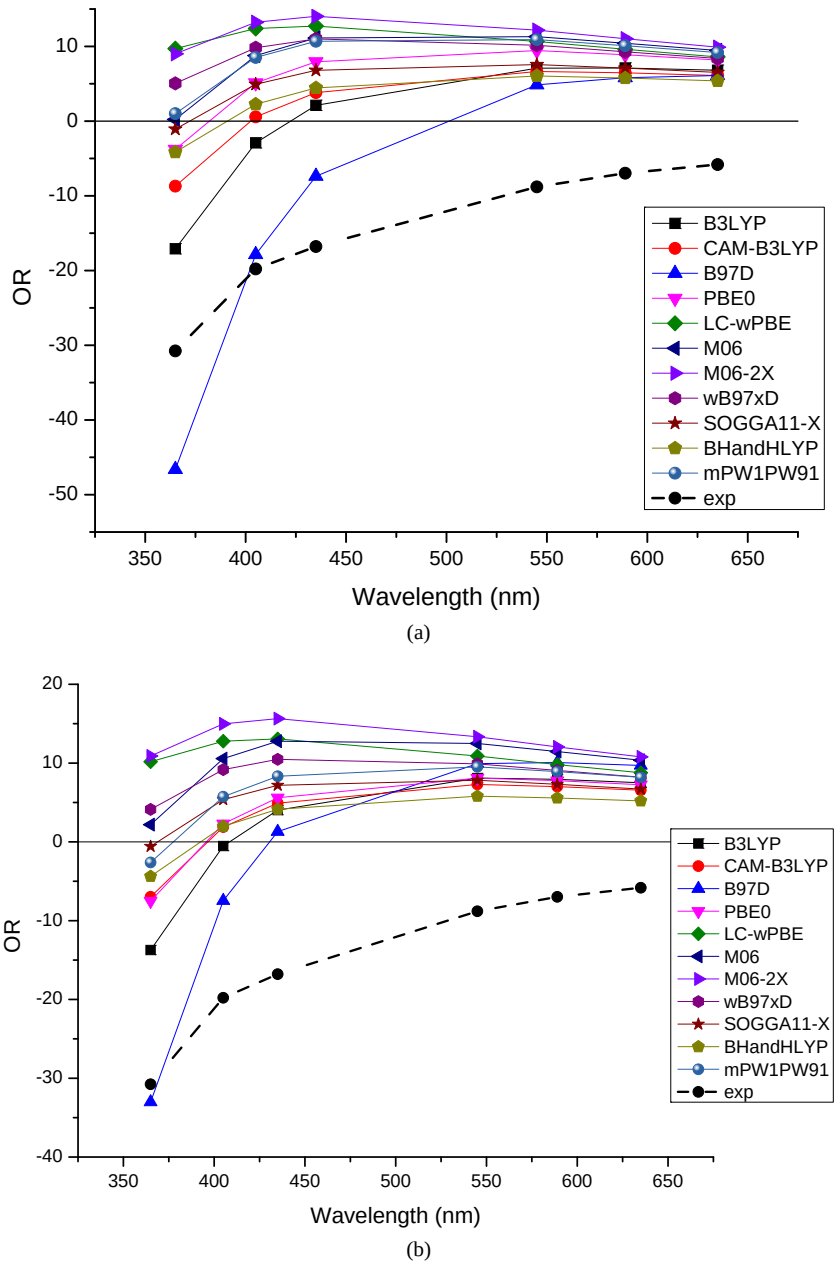

Fig. 2. ORD of (R)-methyloxirane in aqueous solution as calculated by exploiting the PCM and different functionals with the aug-cc-pVDZ basis set. (a): fixed B3LYP/aug-cc-pVDZ/PCM geometry; (b): optimized geometry with each functional. The experimental ORD curve taken from Ref. [46] is also shown.

#225483 - $15.00 USD Received 27 Oct 2014; revised 28 Nov 2014; accepted 28 Nov 2014; published 23 Dec 2014

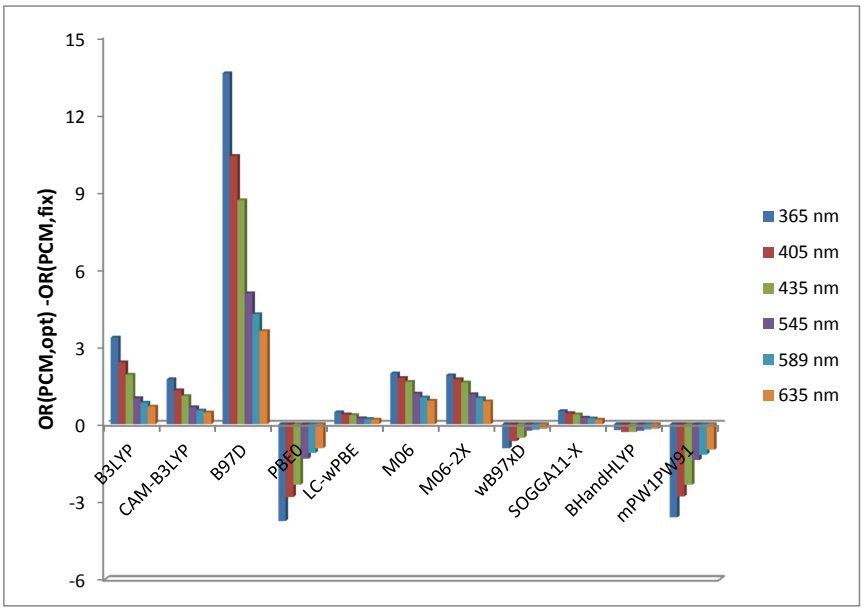

Fig. 3. Difference between OR PCM values calculated with the optimized geometry with each functional and the geometry used in the MD simulation.

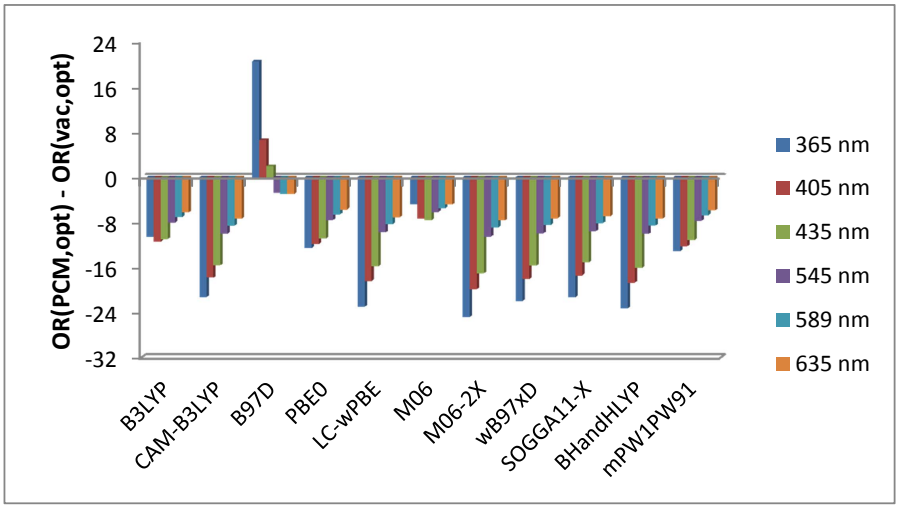

Fig. 4. Difference between OR PCM and gas phase values, at the respective equilibrium geometries.

#225483 - $15.00 USD Received 27 Oct 2014; revised 28 Nov 2014; accepted 28 Nov 2014; published 23 Dec 2014

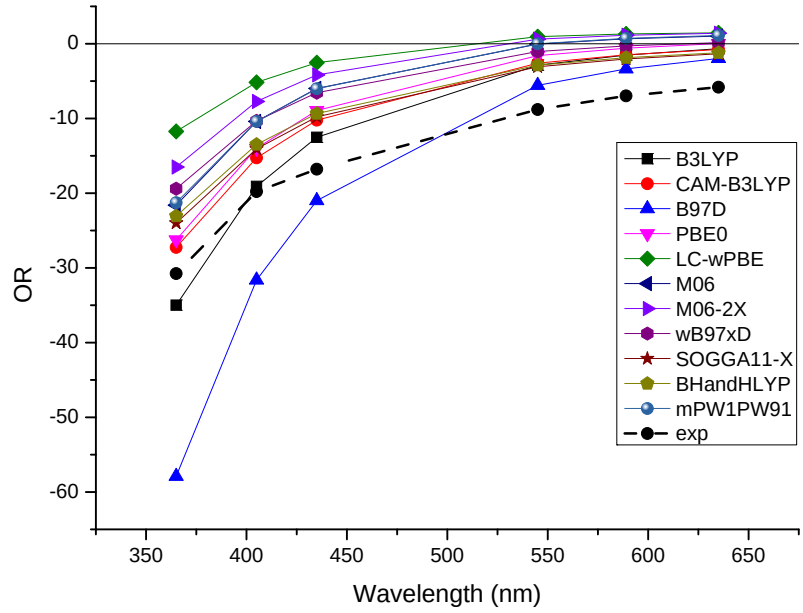

(a)

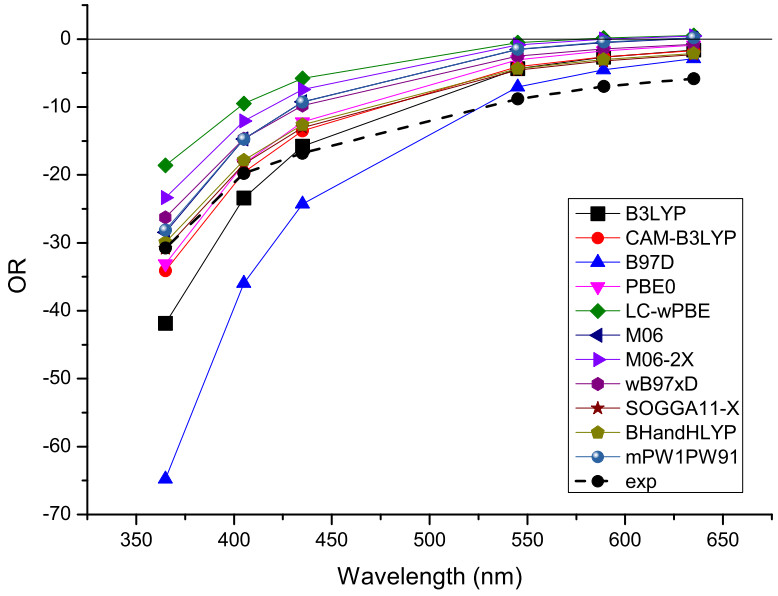

(b)

Fig. 5. ORD of (R)-methyloxirane in aqueous solution as calculated by exploiting the FQ/PCM approach and different functionals with the aug-cc-pVDZ basis set. (a): electronic contribution only; (b): vibrationally averaged values. The experimental ORD curve taken from Ref. [46] is also shown.

#225483 - $15.00 USD Received 27 Oct 2014; revised 28 Nov 2014; accepted 28 Nov 2014; published 23 Dec 2014

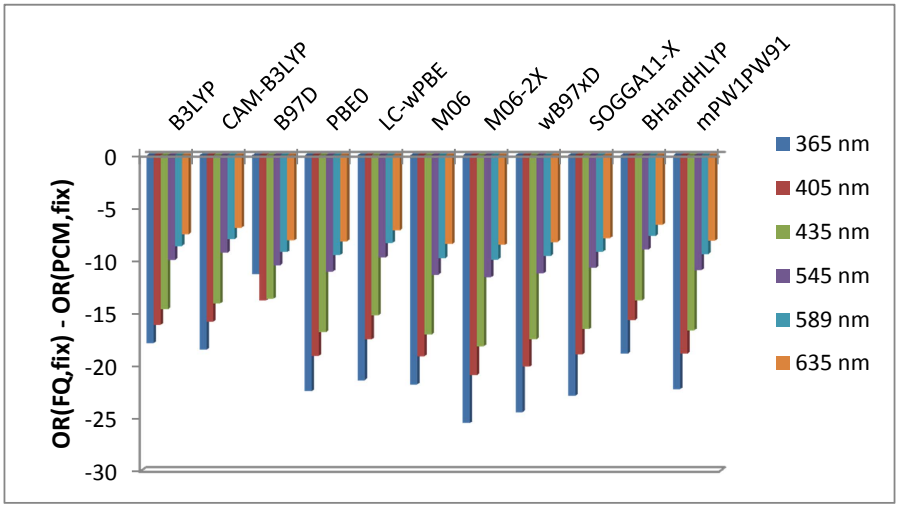

Fig. 6. Difference between OR QM/FQ/PCM (Fig. 5(a)) and PCM (Fig. 2(a)) values calculated with the geometry used in the MD simulation.

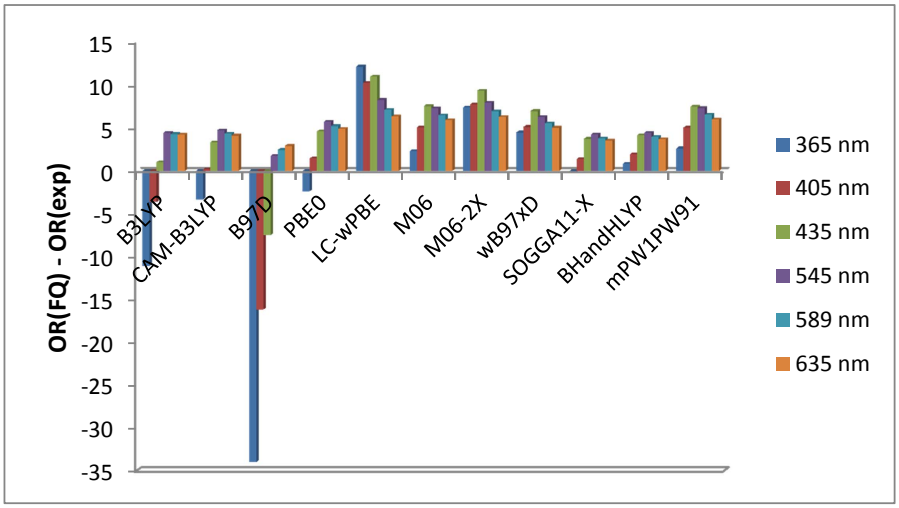

Fig. 7. Difference between OR QM/FQ/PCM (Fig. 5(b)) and experimental values, taken from Ref. [46].

#225483 - $15.00 USD Received 27 Oct 2014; revised 28 Nov 2014; accepted 28 Nov 2014; published 23 Dec 2014

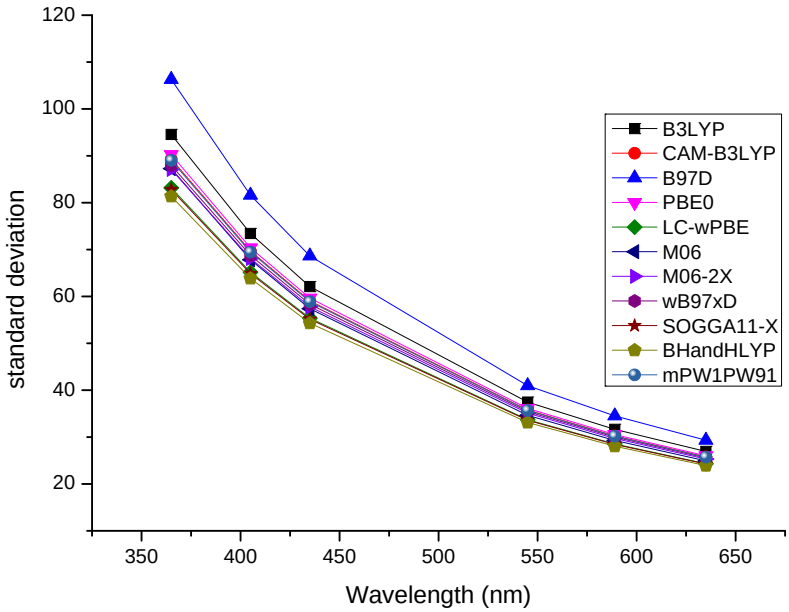

Fig. 8. Standard Deviation of purely electronic QM/FQ/PCM OR values of (R)-methyloxirane in aqueous solution across each snapshot.

same vibrational corrections for all functionals, the standard deviation would not be affected by their introduction. The comparison with the values shown in Fig. 5(a) shows that, as previously reported for B3LYP and CAM-B3LYP [23], the variation of the values around their average is quite substantial. In particular, it ranges from 25 at 635 nm to 90 at 365 nm. This demonstrates that the resorting to super-molecule approaches, which would imply the definition of clusters composed of methyloxirane surrounded by few explicit water molecules, possibly immersed in the PCM dielectric continuum, and treated quantum-mechanically, could be very inaccurate, even though they have been successfully applied to model other properties and other systems [65–69]. In fact, in our case this approach would lead to a limited ensemble of clusters, which would very roughly represent the configurational freedom of water molecules around to the target system. The resulting OR values would fall within a huge range of positive and negative values, almost randomly, and the lack of any accurate averaging of solvent configurations would cause the final value to reproduce very roughly the experimental findings. From our results it also emerges that this huge variance of the OR values of the single snapshots leads to very similar mean values for almost all functionals. Although the value of the single snapshot can be different for different functional, this is not really relevant to the final value. The same could not apply to supermolecule approaches.

In summary, the overall picture that emerges from these results is that the effect of the solvent, introduced by either PCM or, far more accurately, by exploiting the FQ/PCM scheme, is much more significant than the effect of the functional itself, as seen from the similarities between the ORD curves obtained with the ten different hybrid functionals considered in this work.

4. Summary and Conclusions

We have reported on the performance of 11 different Density Functionals, coupled either to implicit PCM or mixed implicit-explicit QM/FQ/PCM approaches, to model the ORD of (R)-methyloxirane in aqueous solution. Our results confirm the inadequacy of implicit solvation

#225483 - $15.00 USD Received 27 Oct 2014; revised 28 Nov 2014; accepted 28 Nov 2014; published 23 Dec 2014

approaches to this property for this system, of which the sign is incorrectly reproduced by the PCM. The data obtained by including specific solute-solvent effects in the computational approach via the QM/FQ/PCM model confirm what was already shown by some of us [23], i.e. that such effects play a major role in the determination of the final property. The overall picture that emerges is that the effect of the solvent is much more significant than the effect of the functional. In fact all the chosen hybrid functionals give a reasonably good agreement with experiments, especially at lower wavelengths, if vibrational corrections are included. Also, a careful averaging over a large number of different solvent configurations around the solute is needed to achieve an accurate reproduction of the experimental results.

Acknowledgments

CC acknowledges support from the Italian MIUR PRIN 2012 NB3KLK_002 and FIRB 2010-Futuro in Ricerca: protocollo: RBFR10Y5VW. The high performance computing facilities of the DREAMS center (http://dreamshpc.sns.it) are acknowledged for providing computer resources. The support of COST CMTS-Action CM1002 Convergent Distributed Environment for Computational Spectroscopy (CoDECS) is also acknowledged. IC acknowledges Compunet of IIT for financial support.